Eur Radiol (2009) 19: 1582–1594
DOI 10.1007/s00330-009-1352-3

S. Trattnig
S. Domayer
G. W. Welsch
T. Mosher
F. Eckstein

MR imaging of cartilage and its repair in the knee - a review

Received: 3 September 2008
Revised: 20 January 2009
Accepted: 26 January 2009
Published online: 13 March 2009

S. Trattnig (✉) · S. Domayer · G. W. Welsch
MR Centre of Excellence,
Department of Radiology,
Medical University Vienna,
Vienna, Austria
e-mail: siegfried.trattnig@meduniwien.ac.at
Tel.: +431-40-4006460
Fax: +431-40-4006475

S. Domayer
Department of Orthopedics,
Medical University Vienna,
Vienna, Austria

T. Mosher
Department of Radiology and Orthopaedic Surgery, Penn State University, College of Medicine,
Hershey, PA, USA

F. Eckstein
Institute of Anatomy & Musculoskeletal Research,
Paracelsus Medical University,
Strubergasse 21,
A5020 Salzburg, Austria

F. Eckstein
Chondrometrics GmbH,
Ulrichshöglerstr. 23,
83404 Ainring, Germany

Abstract Chondral injuries are common lesions of the knee joint, and many patients could benefit from cartilage repair. Widespread cartilage repair techniques require sophisticated noninvasive follow-up using MRI. In addition to the precise morphological assessment of this area of cartilage repair, the cartilage's biochemical constitution can be determined using biochemical MRI techniques. The combination of the clinical outcome after cartilage repair together with the morphological and biochemical description of the cartilage repair tissue as well as the surrounding cartilage can lead to an optimal follow-up evaluation. The present article on MR imaging techniques of cartilage repair focuses on morphological description and scoring using techniques from conventional 2D through advanced isotropic 3D MRI sequences. Furthermore the ultrastructure of the repair tissue and the surrounding cartilage is evaluated in-vivo by biochemical T1-delayed gadolinium enhanced MRI of cartilage (dGEMRIC), T2 relaxation, and diffusion-weighted imaging techniques.

Keywords MRI · Cartilage repair · T2 mapping · dGEMRIC · Diffusion-weighted imaging

Introduction

Chondral injury is a frequent cause of pain and knee-function limitation. The very limited capability for self-repair and subsequent degeneration of injured cartilage and other articular tissues often lead to osteoarthritis, which may eventually result in the need for total knee arthroplasty [1]. Surgical options for cartilage repair in the knee aim to ease clinical symptoms and to postpone the onset of osteoarthritis. Cartilage repair surgery is a highly dynamic

research field, and there is a pressing need for reliable and objective monitoring in order to evaluate and compare various surgical treatment options. The advent of high field MRI and the introduction of knee coils in clinical use yields new technologies for the noninvasive and objective assessment of cartilage repair tissue. This article gives a short survey of the surgical treatment options of cartilage defects and subsequently reviews the state of the art of morphological MRI as well as recent advances in molecular imaging of cartilage repair in the knee.

Cartilage repair surgery

The surgical treatment of chondral defects has the goal of placing repair tissue into the defect in order to stabilize the adjacent native cartilage. Various approaches to achieve defect filling have been conducted and currently include bone marrow-stimulation techniques such as microfracture (MFX) [2–11], osteochondral graft transplantation (mosaicplasty, osteochondral autograft transfer system) [12–14], and autologous chondrocyte implantation (ACI) [15–21].

Microfracture has been shown to be an efficient one-step procedure but produces mainly fibrous repair tissue with an incomplete filling of the defect and limited load-bearing capacity [22–24]. In osteochondral graft transplantation (OAT), osteochondral plugs are taken from non-weight-bearing areas in the femoral condyles or areas that less frequently bear weight using a cylindrical cutting device and are implanted as a mosaic to fill the defect(s). OAT is limited with respect to the size of the defect (maximum= 4 cm^2) that can be filled because (1) only a limited number of grafts are available, (2) in a large defect, the fixation of the grafts becomes instable and may result in uneven surfaces, and (3) impairment due to the mechanical forces during implantation may injure the cartilage layer of the osteochondral plug [25].

ACI requires the excision of a periosteal flap to keep the injected cultured autologous cell suspension in situ. ACI has been applied to 30,000 patients worldwide [18, 19], however, cartilage overgrowth and delamination or fibrous degeneration of the newly formed tissue in 2.4–20% have been observed [26, 27]. As a consequence, there is substantial interest in improving ACI. New ACI techniques are often referred to as scaffold-guided or matrix-associated ACI (MACI) since biomaterials based on collagen [28–30], hyaluronan [31–34], or polylactides [35] are used as scaffolds for cell growth. MACI is less invasive and can be performed arthroscopically in central-anterior defects of the femoral condyle. Moreover, it is applicable to treat defects of up to 10 cm^2 [33, 36–39]. An additional advantage may be more efficient redifferentiation of chondrocytes and hence the formation of hyaline-like repair tissue [40].

MR imaging

Magnetic resonance imaging (MRI), radiological scoring systems, and quantitative image analysis technology have recently started to provide a wealth of new information on articular cartilage and other articular tissues under physiological and patho-physiological conditions. These techniques have been applied to the study of healthy joints and to those suffering from traumatic and degenerative disease.

Given superior tissue contrast and sensitivity to tissue composition, MRI has tremendous potential in the study of cartilage repair. Specifically it may (1) help to estimate the size, nature, and location of lesions preoperatively, in order to optimize surgical planning, (2) help to evaluate the quality and success of tissue repair processes after surgical treatment, and (3) allow one to monitor degenerative changes in the joint after cartilage repair, potentially in comparison to patients who have not been treated for cartilage lesions.

Preoperative estimation of lesion size, nature, and location

MR technique and sequences

MRI assessment of cartilage repair requires cartilage-sensitive sequences such as fat-suppressed three-dimensional gradient echo (3D-GRE) and proton-density (PD) and T2-weighted (dual) fast spin echo (FSE) techniques with or without fat-suppression. In general, 3D-GRE sequences with fat suppression allow the exact depiction of the thickness and surface of cartilage, whereas dual FSE sequences outline the normal and abnormal internal structure of hyaline cartilage [12–15]. Recently developed high-resolution three-dimensional (3D) isotropic cartilage-sensitive sequences at 3 Tesla will further improve the assessment of quantitative morphologic aspects of volumetric cartilage, in particular segmentation and volumetric measurements [41].

Using a model of artificial cartilage lesions in rabbit joints, it was shown that the ability to detect small cartilage lesions critically depended on the spatial resolution of the imaging sequence, and that achieving a high resolution justified some degree of sacrifice in signal-to-noise ratios (SNR) and contrast-to-noise ratios (CNR) [42]. Rubenstein et al. [43] demonstrated that a voxel size under 300 μm is required to reveal fraying of the articular surface of cartilage. High-field MRI scanners increase the possibilites of 3D imaging; GRE images yield high resolution in-plane and thin slices with a sufficient signal-to-noise ratio, while scan times can be kept well below 10 min. New coil technologies with multi-element design allow the use of parallel imaging, which can additionally decrease the scan time by a factor of two to three.

Scoring methods

Most scoring methods for articular cartilage lesions grade lesion severity from 0–3 or 4 based on subjective evaluations and commonly differentiate between cartilage lesions of less than 50% depth, more than 50% depth, and full thickness. Peterfy et al. [44] have described a comprehensive MRI scoring system (WORMS = whole-organ MRI scoring), in which numerous features (cartilage signal and morphology, subchondral bone marrow abnormalities, meniscal and ligmament changes, etc.) are graded within the knee. The interobserver agreement among two trained readers was high (intraclass correlation coefficient >0.98 for cartilage abnormalities and >0.80 for most features, except for bone attrition and synovitis) using a 1.5 T whole-body magnet. Another compartment-based scoring system termed knee osteoarthritis scoring system (KOSS) has also been published, with intraobserver reproducibility of 0.76–0.96 (ICC) and interobserver reproducibility (intraclass correlation coefficient) amongst two independent observers of 0.63–0.91 [45].

Some limitations of these scoring systems have recently been identified [46] when applying the WORMS grading systems to knees of 336 subjects (three readers) and comparing these with a Rasch measurement model. The authors commented that adding up individual scoring subscales, as recommended by WORMS, is problematic, and that several subscales (in particular those for cartilage signal and morphology and for osteophytes) may need to be redeveloped.

In a recent report [47], the reliability of a novel MRI scoring system for evaluating osteoarthritis (OA) of the knee was explored. Nine intra-articular anatomical divisions and eight items were tested, including features of cartilage, bone-marrow lesions (BML), osteophytes, synovitis, effusions, and ligaments, and a scaling of 0–3 was applied for each of these to yield the Boston-Leeds Osteoarthritis Knee Score (BLOKS). A series of iterative reliability exercises was performed to reduce the initial items. The interreader reliability for the final BLOKS items ranged from 0.51 for meniscal extrusion up to 0.79 for meniscal tear, with that for cartilage morphology being 0.72. In another sample, both BLOKS and WORMS were used to score BML. Maximum BML size in BLOKS had a positive linear relation with VAS pain, whereas in WORMS it did not. Baseline BML was associated with cartilage loss on both the BLOKS and WORMS scale, but the association was stronger for BLOKS than for WORMS.

Accuracy of MRI for chondral lesions—in vitro and in vivo studies

Satisfactory specificity and sensitivity for detecting chondral lesions have been demonstrated in knee specimens and in vivo with arthroscopic verification [48–54]. Bredella et al. [55] reported a sensitivity of 93% and a specificity of 99% in detecting chondral lesions with MRI versus athroscopy when axial and coronal images were combined, and values of 94 and 99% when images in all three planes were used. In that study, accuracy was highest for severe cartilage lesions and lowest for smaller lesions, particularly for signal intensity alterations.

Using a porcine model of artificial cartilage lesions [56], the highest lesion detection rate was found with an intermediate-weighted FSE sequence at 3.0 T (90 vs. 62% at 1.5 T), whereas the lesion grade was most accurately evaluated with SPGR at 3.0 T (83 versus 70% at 1.5 T). Receiver operator characteristics (ROC) analyses in the same model confirmed improved diagnostic performance in detecting cartilage lesions at 3.0 T if high-resolution imaging protocols (slice thickness ≤2 mm and in-plane resolution ≤0.39 mm) were used [57]. Quantitative measurements of cartilage lesion depth, diameter, area, and volume have been validated in a porcine experimental model of OA [58]. In human knee cartilage, the mean difference between measured and actual artificial cartilage defect diameters was reported to be <0.1 mm, whereas the lesion depth was underestimated in MRI by >0.4 mm [59]. Graichen et al. [60] reported an overestimation of the true size of artificial cartilage defects in the human knee, which decreased from 42% in 3-mm defects to 4% in 8-mm defects.

Evaluation of the quality of tissue-repair processes after surgical treatment

This has been the area of the most intense use of MRI in cartilage repair and has thus received the widest interest. The MR sequences commonly used for evaluating cartilage repair morphologically are identical with those that have been used for evaluating cartilage lesions as described above (Figs. 1, 2). Figures 1 and 2 show high-resolution MR images of cartilage repair tissue at different time intervals after surgery (6 vs. 60 months).

The evaluation of the success of cartilage repair procedures [61–66] requires specific grading systems, one of which is MOCART [62–64, 67]. The validity and reliability of this system has been evaluated for the assessment of matrix-associated autologous chondrocyte transplantation (MACI) in the knee [62], using nine pertinent variables. These included filling of the defect, integration of the border zone to the adjacent cartilage, intactness of the subchondral lamina, intactness of the subchondral bone, relative signal intensities of the repair tissue compared to the adjacent native cartilage, and others. An almost perfect agreement between readers (ICC >0.81) was found for eight of the nine variables. When comparing the MRI scores with clinical outcome (knee-related quality of life) 2 years after ACT, a statistically significant correlation was found for “filling of the defect,” “structure of the

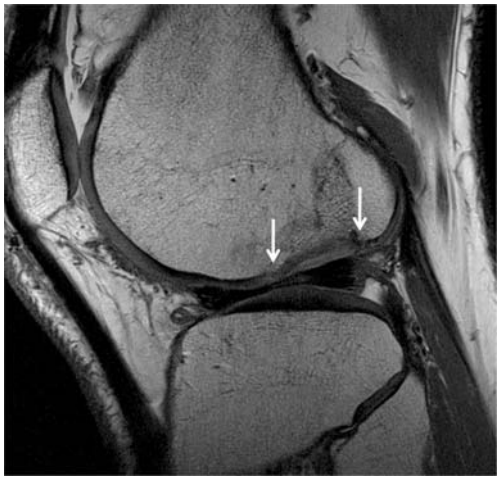

Fig. 1 Sagittal high-resolution (0.23×0.23×2 mm) proton-density turbo spin echo (PD TSE) 6 months after matrix-associated autologous chondrocyte implantation (MACI) (area of cartilage repair marked with *arrows*) of the lateral femoral condyle (LFC)

repair tissue," "changes in the subchondral bone," and "signal intensities of the repair issue."

In addition to morphologic imaging, quantitative MRI techniques give the option of studying the composition of the cartilage matrix ultrastructure and can therefore be considered molecular-imaging techniques [68]. These techniques are of particular interest for the study of cartilage repair as they have the potential to evaluate cartilage maturation and adaptation after surgery in vivo [63, 67, 69–71]. The most promising techniques in this context include the transverse relaxation time T2, the longitudinal relaxation time T1 in the presence of gadolinium ($T1_{Gd}$ = dGEMRIC index), and diffusion-weighted imaging.

It has to be emphasized that while much of the initial validation research for these functional cartilage imaging techniques was performed on cartilage tissue, there has been so far limited validation of these techniques in cartilage repair tissue.

Measurement of T2 in cartilage

The majority of cartilage T2 mapping studies have used conventional multislice multi spin echo (MSME) sequences, typically with a minimum of seven echoes. The in vivo precision errors of the technique have been reported recently [72]. Measurements of T2 of articular cartilage provide a potential imaging biomarker of structural changes in the collagen matrix [73]. Perturbation of the collagen architecture leads to increased T2-weighted signal intensity, whereas sites of decreased signal intensity can be observed adjacent to sites of focal cartilage injury [74]. While increased cartilage T2 is associated with an increase in water content [75] and a decrease in collagen content [76], the dominant factor influencing regional variation in T2 appears to be the anisotropic arrangement of the type II collagen matrix [77, 78]. Dardzinski et al. [79] concluded that the T2 characteristics in cartilage are strongly influenced by the orientation of the collagen framework and that the dipole-dipole interaction anisotropy in the presence of restricted water mobility has an important influence on spin-spin relaxation in the deep layers of cartilage. Additionally in-vitro T2 relaxation studies and animal studies have also demonstrated a close relationship between T2 and the architecture of collagen [80–82].

A recent study has observed a strong inverse correlation of fiber anisotropy determined with polarized light microscopy and the T2 of the cartilage [83].

Whereas the sensitivity of T2 to cartilage degeneration in osteoarthritis is yet unclear, the sensitivity of T2 to collagen architecture has been successfully applied to study maturational changes in the collagen matrix of osteochondral plugs from juvenile animals [83–85] and age-related changes in mature cartilage [86–88].

T2 mapping in cartilage repair

The line profiles of T2 relaxation times as suggested by Mosher and Dardzinski [79, 87] provide a very helpful insight into the maturation process of cartilage repair tissue over time and facilitate a comparison with native healthy cartilage. The extracellular matrix of native articular cartilage is shaped by a highly organized collagen network, which varies across the histological zones of normal hyaline articular cartilage tissue [1]. Under ideal circumstances, cartilage repair tissue produced following cartilage repair techniques, should, over time, develop a collagen network with a similar shape, collagen concentration, and in particular, a similar zonal organization as normal hyaline cartilage.

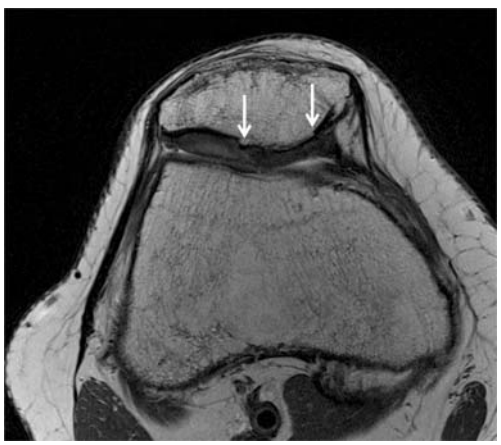

Fig. 2 Axial high-resolution (0.23×0.23×2 mm) proton-density turbo spin echo (PD TSE) 60 months after matrix-associated autologous chondrocyte implantation (MACI) of the patella (*arrows*)

In a recent study by White et al. [89], normal hyaline cartilage and cartilage repair tissue were differentiated by zonal T2 mapping in equine subjects. Arthroscopic OAT and MFX were performed and evaluation of zonal T2 variation showed a characteristic distribution across the depth of the cartilage in control and OAT sites, with low T2 values near the subchondral bone and higher T2 values near the cartilage surface [89]. However no zonal variation was found within MFX repair tissue. T2 measurement results in this study were correlated with histology and collagen structural anisotropy as assessed by polarized light microscopy. OAT and normal hyaline cartilage sites illustrated a normal zonal collagen organization, whereas MFX showed disorganized fibrous reparative tissue [89].

Welsch et al. [90] evaluated T2 in-vivo in normal hyaline cartilage sites and in cartilage repair tissue after MFX and MACI in humans. Similar to the in vivo animal study of White et al. [89], no differences between deep and superficial layers of cartilage repair tissue were observed after MFX. After MACI, a characteristic zonal variation in mean T2 measurements was observed, but compared to healthy cartilage, the increase in mean T2 values from the deep to the superficial zones was less pronounced (Fig. 3a, b). These results suggest differences in quantitative T2 mapping results between MFX and MACI, possibly reflective of collagen and/or water concentration and organization. Taking into account that histological biopsies obtained at postoperative follow-up arthroscopy have reported more fibrocartilage after MFX [91] and more "hyaline-like" cartilage after MACI [37], these findings indicate that quantitative T2 mapping may provide information on the specific structure of different cartilage repair tissues.

In another study, clinical scores were correlated with T2 values in patients after microfracture [92]. The knees of 24 patients were studied after a mean postoperative interval of 29 months using 3T MRI. An individual relative T2 index was calculated by expressing the mean T2 of the repair tissue as a percentage of mean T2 of normal, hyaline cartilage. The T2 index correlated with the clinical outcome of the Lysholm Score and the IKDC Subjective Knee Evaluation Form.

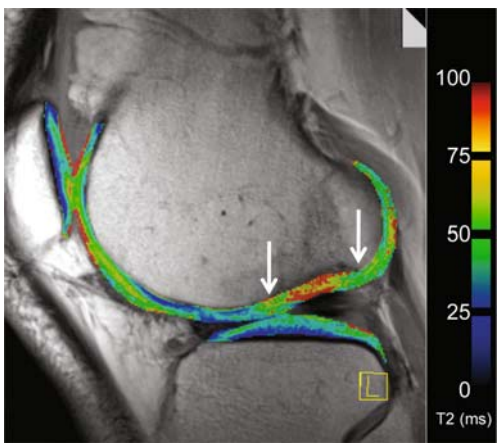

Fig. 3 Axial T2 maps of the patella 60 months after matrix-associated autologous chondrocyte implantation (MACI) (**a**) (same patient as Fig. 2) and 36 months after microfracture (MFX) (**b**)

Using quantitative global T2 mapping of patients at different postoperative intervals after MACI surgery, significantly higher T2 values were found in cartilage repair tissue in the early stage (3–13 months) after surgery in an intraindividual comparison with native hyaline cartilage [69] (Fig. 4). Furthermore, a decrease in repair-tissue T2 values was observed over time, with the T2 values becoming similar to native healthy cartilage. This finding was in agreement with a study by Kurkijarvi et al. [93] who, using 1.5 T, reported T2 values in the repair tissue and normal hyaline cartilage of 60±10 and 50±7 ms, respectively, in 10 patients at 10–15 months after ACI surgery. The zonal variation in repair tissue [69] has been demonstrated through analysis of the T2 line profiles showing the variation in T2 values from the subchondral bone to cartilage surface. With increasing postoperative interval the shape of the T2 line profiles (and the calculated T2 line profile values) was found to become similar to the reference healthy cartilage sites [69].

After MFX, significantly lower global mean T2 values of cartilage repair tissue were found whereas after MACI no significant change in mean T2 values was observed compared to morphologically normal control sites [90]. These findings imply that the composition of the repair tissue created with the two procedures is different.

Feasibility in clinical routine and diagnostic value

T2 mapping can be easily implemented in clinical routine MRI. The duration of T2 mapping sequences at 3 T is approximately 6 min, and contrast agent is not required.

T2 is highly sensitive to alterations of the cartilage matrix; free water, collagen concentration, and the orientation of the collagen fibrils affect T2 values. T2 may differ significantly among healthy individuals. In cartilage repair patients, it is therefore important to consider T2 of the adjacent hyaline cartilage in the evaluation of the repair tissue.

Valuable data result from the zonal variation of the repair tissue. T2 can assess the repair tissue organization and also visualize tissue remodeling over time. This may be considered the main strength of T2 mapping rather than the assessment of absolute values.

Delayed gadolinium-enhanced MRI of cartilage: dGEMRIC

Glycosaminoglycans (GAG) are the main source of fixed charge density (FCD) in cartilage and have been reported to be lost in the early stage of cartilage degeneration [94]. Intravenously administered gadolinium diethylenetriamine

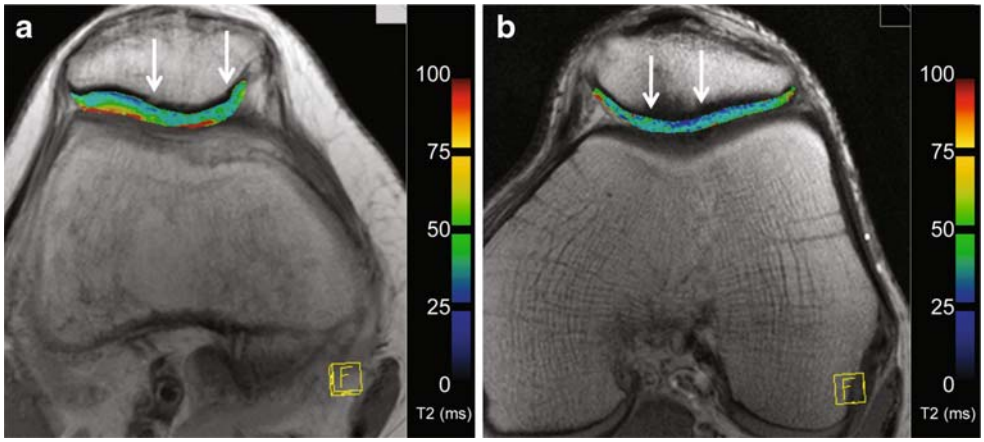

Fig. 4 Sagittal high-resolution (0.42×0.42×3 mm) T2 map of the same patient visualized in Fig. 1 with a follow-up interval of 6 months after matrix-associated autologous chondrocyte implantation (MACI) of the lateral femoral condyle (LFC) (*arrows*)

pentaacetate anion (Gd-DTPA^{2-}) penetrates the cartilage through both the articular surface and the subchondral bone. The negatively charged contrast agent equilibrates in inverse relation to the FCD, which is in turn directly related to the GAG concentration. Therefore T1, which is determined by the Gd-DTPA^{2-} concentration, can be used as a specific measure of tissue GAG concentration. An increased accumulation of contrast agent due to a depletion of GAG in cartilage will lead to decreased T1.

T1 relaxation enhanced by delayed administration of Gd-DTPA^{2-}, the dGEMRIC (delayed gadolinium-enhanced MRI of cartilage) technique, is currently the most widely used method for analyzing proteoglycan depletion in articular cartilage and has provided valuable results in vitro and in vivo [95–99]. Post-contrast T1 mapping is usually performed approximately 90 min after intravenous injection of Gd-DTPA^{2-}, to allow sufficient time for the contrast agent (Gd) to diffuse into the cartilage layer before the images are acquired.

Since standard T1 mapping with inversion recovery is time consuming or limited to single-slice acquisitions, 3D applications of dGEMRIC that provide greater coverage and faster imaging times are currently undergoing validation [100, 101].

dGEMRIC for the assessment of cartilage repair

When evaluating cartilage repair using dGEMRIC, one must take into account that, contrary to studies in normal or degenerative cartilage, the repair tissue shows heterogeneous T1 values compared to normal cartilage prior to the administration of Gd. Thus, postcontrast T1 mapping does not correlate directly with glycosaminoglycan content, but the difference between pre- and postcontrast imaging (delta relaxation rate = $1/T1_{Gd} - 1/T1_{precontrast}$) does [102]. Watanabe et al. [102] demonstrated that the relative delta R1 index (delta relaxation rate of repair tissue divided by the delta relaxation rate of normal hyaline cartilage) correlates with the GAG concentration in repair tissue as measured by gas chromatography, an accepted gold standard for the measurement of GAG content in biopsy samples.

A recent study by Trattnig et al. [70] demonstrated that it is feasible to apply a 3D variable flip angle dGEMRIC technique in patients following MACI surgery to obtain information related to the long-term development and maturation of grafts within clinically acceptable scan times (Fig. 5a, b). In accordance with the study by Watanabe et al. [102], increased T1 values in repair tissue of MACI

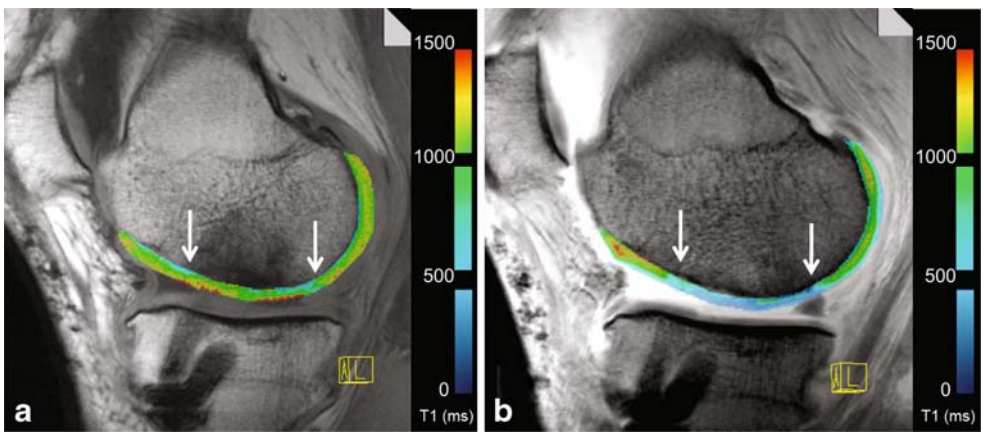

Fig. 5 Sagittal T1-dGEMRIC maps of a patient 36 months after matrix-associated autologous chondrocyte implantation (MACI) of the medial femoral condyle (MFC) before (**a**) and after (**b**) intravenous contrast medium Gd-DTPA^{2-}

patients were found precontrast at all time intervals after surgery. This seems to highlight the necessity of measuring the native T1 values for evaluation of GAG content at the repair site. This is also supported by the results of an in vitro study by Wayne et al. [103] who found that a T1 ratio calculated as $T1_{Gd}$/T1 made it possible to distinguish between collagenase- and chondroitase-treated cartilage, whereas, while the $T1_{Gd}$ values alone were significantly different between treated and untreated cartilage, they were not between the two treatments.

Two other studies reported that dGEMRIC has potential as a noninvasive MR imaging technique for monitoring the GAG content after ACI [93, 104]. The findings of both studies suggest that the GAG concentration in repair cartilage at month 10 (or longer) after ACI is comparable to the GAG concentration in the adjacent normal hyaline cartilage. However the authors performed MR imaging only after intravenous contrast medium application and may thus have overestimated the GAG content in the repair tissue.

In contrast to these studies, Trattnig et al. [70] aimed to assess the maturation of cartilage implants over time. As it is known from biopsy studies that most of the changes in cartilage implants occur in the early postoperative period. Patients were subdivided into early and late postoperative groups (3–13 months and 19–42 months, respectively). The mean R1 (in 1/s) for repair tissue was 2.49±1.15 versus 1.04±0.56 at the intact control site in the early postoperative group and 1.90±0.97 compared to 0.81±0.47 in the late postoperative group. The difference between repair tissue and normal hyaline cartilage was statistically significant ($P<0.007$) in both groups, but the difference between repair tissue and normal hyaline cartilage between the groups was not ($P=0.205$). The mean relative relaxation rate R1 was 2.40 in the early group and 2.35 in the late group.

A possible explanation for these results comes from histological investigations of biopsies. These have shown that patients with MACI develop hyaline-like repair tissue over time, whilst in patients with microfracture fibrous tissue predominates [27, 105]. dGEMRIC has been used to evaluate relative glycosaminoglycan (GAG) content of repair tissue in patients after different surgical cartilage repair techniques such as MFX, ACI, and MACI [93] (Fig. 6a, b). In one of these studies [106], 10 patients treated with MFX and 10 with MACI were compared after being matched by age and postoperative interval. The mean delta R1 for MFX was 1.07±0.34 versus 0.32±0.20 at the control site, whereas for MACI it was 1.90±0.49 versus 0.87±0.44. This resulted in a relative delta R1 of 3.39 for MFX and 2.18 for MACI, the difference between the cartilage repair groups being statistically significant.

The repair tissue formed by MFX contained less PGs and an abnormal distribution of collagen compared to normal cartilage (analyzed by histology and biochemistry), which may explain the poor resultant mechanical properties often exhibited by repair tissue [107, 108]. These findings are supported by T1 mapping results that showed a significantly higher relative delta R1 of the repair tissue after MFX than after MACI, suggesting a lower GAG content after MFX.

Feasibility in clinical routine and diagnostic value

The dGEMRIC technique has been demonstrated to be specific for GAG by several investigators [70, 96, 97, 109, 110], and also to be sensitive to the clinical symptoms in patients with hip dysplasia. The recently developed 3D GRE T1 sequences are appropriate for the implementation in clinical MRI protocols. Still, exercise and an interval of approximately 60 min after contrast-agent administration are required to ensure the distribution of Gd-$DTPA^{2-}$ among the negatively charged GAGs. In cartilage repair both pre- and postcontrast measurements are currently considered necessary for a maximum sensitivity of the technique [102]. The resulting overall mesurement time of 2 h diminishes the attractiveness for clinical use. Still, dGEMRIC can be considered to be the current gold

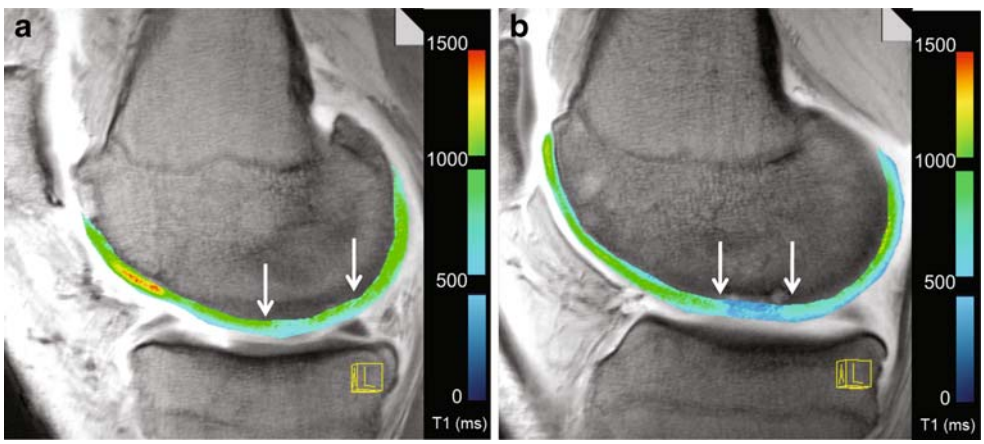

Fig. 6 Sagittal intravenously enhanced T1-dGEMRIC maps of a patient 36 months after matrix-associated autologous chondrocyte implantation (MACI) of the medial femoral condyle (MFC) (**a**) and a patient 36 months after microfracture (MFX) of the MFC (**b**)

standard in cartilage ultrastructure MRI imaging and is valuable for use in clinical studies.

Diffusion techniques in cartilage repair

One encouraging alternative to the techniques mentioned above is diffusion-weighted sequence [111]. Diffusion-weighted imaging (DWI) is based on molecular motion that is influenced by intra- and extracellular barriers. Consequently, it is possible to estimate biochemical structure and architecture of the tissue by measuring molecular movement. When based on spin-echo (SE) sequences, DWI is relatively insensitive to susceptibility effects, but diffusion-weighted SE sequences require acquisition times that cannot be readily applied in clinical practice. Echo planar imaging (EPI)-based diffusion sequences are the current gold standard of DWI in neuro applications, but these suffer from image distortions (susceptibility artifacts) and from limitations in contrast (due to the long echo times required). Both render them impracticable for imaging tissues with short T2, such as cartilage and muscles.

Alternatively, diffusion imaging can be performed using steady-state free precession sequences (SSFP), which provide diffusion weighting at relatively short echo times. This is achieved by the application of a monopolar diffusion sensitizing gradient, which leads to a diffusion weighting of consecutive echoes (spin echoes and stimulated echoes) under steady-state conditions. For the assessment of diffusion-weighted images, a three-dimensional steady-state diffusion technique called PSIF has been used [112]. Note that the PSIF is a time-reversed FISP (fast imaging by steady state precession) sequence. In order to assess diffusional behavior of the cartilage semiquantitatively, the diffusion sequence protocol should consist of two immediately consecutive measurements with 0 and 75 $mT \cdot ms^{-1} \cdot m^{-1}$ monopolar diffusion gradient moments for DWI, but identical imaging parameters. For evaluation, the quotient image (nondiffusion-weighted/diffusion-weighted image) is calculated on a pixel-by-pixel basis.

In a series of 15 patients, the feasibility of diffusion-weighted PSIF imaging after MACI was demonstrated with high resolution in vivo [113] (Fig. 7). The results showed that at follow-up (different time points) the diffusion behavior of the transplants was changing. In the earlier postoperative period (3–13 months), the diffusion was more restricted, but the restriction was lower in the later postoperative period. Even after a period of up to 42 months, there was still a difference in diffusion values between repair tissue and normal hyaline cartilage.

Diffusion-weighted imaging and semi-quantitative analysis can complement the information obtained from approaches that rely on relaxation properties, such as T2-mapping or dGEMRIC. In comparison with dGEMRIC, no contrast medium is needed, the anatomical coverage is larger, the spatial resolution higher, and the scan times shorter. Diffusion therefore is a promising tool for compositional evaluation of cartilage transplants in the future and may be added to dGEMRIC and T2 mapping in a clinical setting for evaluation of cartilage repair outcomes.

Feasibility in clinical routine and diagnostic value

Diffusion-weighted imaging does not require contrast agent, and current sequences take approximately 5 min. The technique therefore is appropriate for clinical routine MRI. A disadvantage is that DWI is not quantitative, and therefore is not as appropriate as T2 mapping or dGEMRIC for the direct comparison of cartilage repair techniques. However, the technique is more sensitive than T2 mapping and might provide information on the nutrition of the repair tissue.

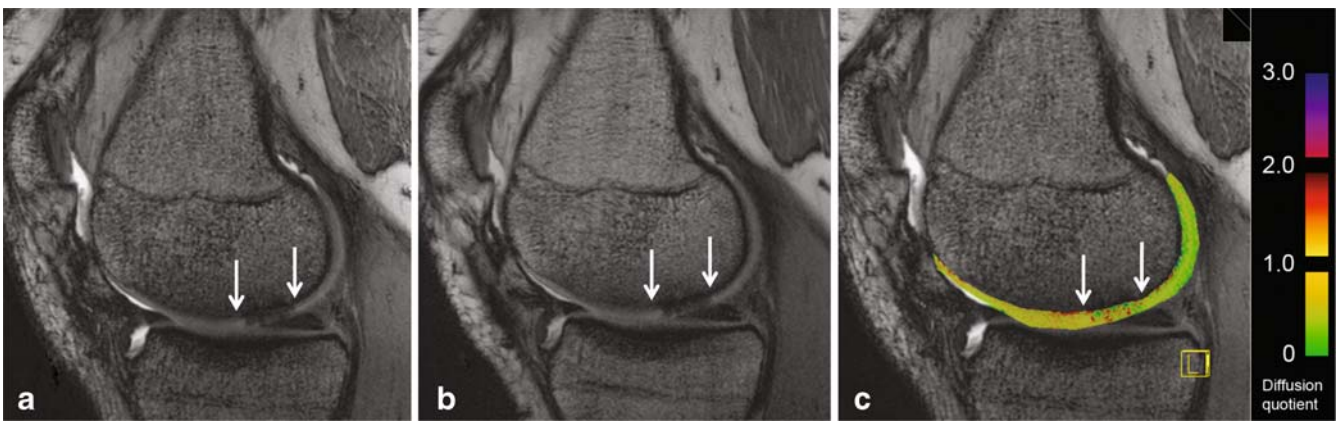

Fig. 7a–c Sagittal diffusion-weighted image (DWI) of a patient 60 months after matrix-associated autologous chondrocyte implantation (MACI) of the medial femoral condyle (MFC) marked by *arrows*. For DWI, a three-dimensional balanced steady-state gradient echo pulse sequence with diffusion weighting (3D-DW PSIF) was used with 0 (**a**) and 75 $mT \cdot ms^{-1} \cdot m^{-1}$ (**b**) monopolar diffusion gradient moments resulting in the divided semi-quantitative DWI map (**c**)

Monitoring degenerative changes in the joint after cartilage repair

In the context of monitoring progression of osteoarthritis (OA), methods for quantitative evaluation of articular cartilage morphology (e.g., volume and thickness) have been widely applied over recent years [114–116]. A nomenclature for MRI-based measurements of cartilage morphology and composition has been proposed [117]. A recent study [118, 119] has evaluated the feasibility of quantitative MRI analysis of cartilage morphology in 21 patients after autologous chondrocyte implantation (ACI). Sagittal fat-suppressed 3D FLASH sequences were obtained pre-ACI surgery and 1-year post-ACI surgery in the femoral condyles. The cartilage volume, mean cartilage thickness, and size of the cartilage-bone interface were determined.

Susceptibility artifacts were a problem in 3 of the 21 patients. The reproducibility error (coefficient of variation %) of cartilage volume measurement was 3.9 and 4.4% for the medial and lateral tibia, respectively, and 5.1% for the femur. A 6% increase in cartilage volume and thickness was observed in the treated femora ($P<0.001$ Wilcoxon) relative to the pre-OP data, but no significant change in the (nonoperated) tibia. Sensitivity to change for femoral cartilage was improved when evaluating only the treated portion of the femur in contrast to the total femur. Morphological cartilage analysis following cartilage repair procedures may help to determine the effectiveness of these procedures to stop degenerative disease progression.

Clinical relevance

The composition of the repair tissue is deemed to be highly significant for the clinical outcome in the long term. Fibrous cartilage repair tissue is subjected to degeneration, which leads to failure [120], and it has been demonstrated that patients with hyaline-like repair tissue after ACI do better than those with fibrous repair tissue [121]. Kreuz et al. found that clinical outcome after microfracture declines after 18 months [24]. Knutsen et al. [22] did not find a significant difference between microfracture and ACI in the knee at 2 years; however, the rate of hyaline-like tissue was higher in ACI biopsies. At 5 years, no significant differences were found either; however, there was no failure in patients with hyaline-like repair tissue [122]. Saris et al. [123] found superior repair tissue after ACI in histologic evaluation 1 year after surgery. Long-term follow-up may show if higher repair tissue quality will be associated with better outcome.

ACI repair tissue quality is subject to a high variability [22, 26, 71, 105, 121, 124]. This apparently also applies to MACI [38, 125], but while various MACI techniques are in clinical use, there are few data regarding MACI repair-tissue composition.

Due to its noninvasive nature and its reproducibility, MRI has a substantial potential to evaluate the efficacy of different cartilage repair techniques. The feasibility of taking equivalent measurements at different sites if a common MRI unit configuration is adhered to also gives the option for use in multicenter studies. This may be of importance since it is difficult to obtain high numbers of patients at a single site. The possibility of direct evaluation of GAG content of the repair tissue may shorten the follow-up period that is needed to determine the efficacy of a certain technique, since low GAG at short-term follow-up will discourage clinicians from pursuing treatment. Patients might therefore see a direct benefit from molecular MRI imaging of cartilage repair.

MRI additionally gives a very precise estimate of progressing degeneration and will be essential for objectively assessing the long-term outcome of cartilage repair.

Conclusion

Exciting technologies have been developed recently for evaluating cartilage repair in vivo. A challenge, however, remains demonstrating that cartilage repair can prevent joint degeneration, preferably in prospective randomized controlled trials, and clinical validating imaging outcomes, that is the correlation of imaging biomarkers with how a patient feels and functions [3–7, 62]. Whereas morphological assessment has been used to score or measure cartilage lesion size and location, to determine cartilage deformational behavior in vivo and to look at the effect of cartilage repair on cartilage volume/thickness loss with time, compositional MR imaging techniques including T2, dGEMRIC, and diffusion are most promising in studying cartilage tissue maturation after repair.

There are marked differences in the structure and composition of repair tissue based on the method of repair as well as temporal changes as the tissue matures. Because these tissue properties have substantial influence on the relaxation and diffusion of water in the tissue, results of functional cartilage imaging such as T2 mapping, dGEMRIC, and diffusion are likely to be different from mature cartilage tissue. Additional research and validation is needed to guide interpretation of the results of these techniques as they are applied to the study and monitoring of cartilage repair. Future studies will also be needed to determine whether MRI is prognostic of clinical outcome and can replace arthroscopic biopsy for monitoring repair-tissue histology. The major challenge thus is not only in the continued technical improvement of these tools, but in validating their correlation with structural and clinical outcome.

Acknowledgements Funding for this study was provided by Austrian Science Fund (FWF) FWF-TRP-Projekt L243-B15 and FWF project: P18110 B15.

References

1. Buckwalter JA, Mankin HJ (1998) Articular cartilage: degeneration and osteoarthritis, repair, regeneration, and transplantation. Instr Course Lect 47:487–504
2. Steadman JR, Rodkey WG, Rodrigo JJ (2001) Microfracture: surgical technique and rehabilitation to treat chondral defects. Clin Orthop Relat Res: S362–S369
3. Raynauld JP, Martel-Pelletier J, Berthiaume MJ et al (2006) Long term evaluation of disease progression through the quantitative magnetic resonance imaging of symptomatic knee osteoarthritis patients: correlation with clinical symptoms and radiographic changes. Arthritis Res Ther 8:R21
4. Conaghan PG, Felson D, Gold G et al (2006) MRI and non-cartilaginous structures in knee osteoarthritis. Osteoarthr Cartil 14(Suppl A):A87–A94
5. Cicuttini FM, Jones G, Forbes A et al (2004) Rate of cartilage loss at two years predicts subsequent total knee arthroplasty: a prospective study. Ann Rheum Dis 63:1124–1127
6. Torres L, Dunlop DD, Peterfy C et al (2006) The relationship between specific tissue lesions and pain severity in persons with knee osteoarthritis. Osteoarthr Cartil 14:1033–1040
7. Zhai G, Blizzard L, Srikanth V et al (2006) Correlates of knee pain in older adults: Tasmanian Older Adult Cohort Study. Arthritis Rheum 55:264–271
8. Steadman JR, Briggs KK, Rodrigo JJ et al (2003) Outcomes of microfracture for traumatic chondral defects of the knee: average 11-year follow-up. Arthroscopy 19:477–484
9. Steadman JR, Miller BS, Karas SG et al (2003) The microfracture technique in the treatment of full-thickness chondral lesions of the knee in National Football League players. J Knee Surg 16:83–86
10. Steadman JR, Rodkey WGBriggs KK (2002) Microfracture to treat full-thickness chondral defects: surgical technique, rehabilitation, and outcomes. J Knee Surg 15:170–6
11. Steadman JR, Rodkey WG, Briggs KK et al (1999) [The microfracture technique in the management of complete cartilage defects in the knee joint]. Orthopade 28:26–32
12. Jakob RP, Franz T, Gautier E et al (2002) Autologous osteochondral grafting in the knee: indication, results, and reflections. Clin Orthop Relat Res 401:170–184
13. Hangody L, Feczko P, Bartha L et al (2001) Mosaicplasty for the treatment of articular defects of the knee and ankle. Clin Orthop Relat Res 391 (Suppl):S328–S336
14. Bobic V (1999) [Autologous osteochondral grafts in the management of articular cartilage lesions]. Orthopade 28:19–25
15. Brittberg M, Lindahl A, Nilsson A et al (1994) Treatment of deep cartilage defects in the knee with autologous chondrocyte transplantation. N Engl J Med 331:889–895
16. Petersen L, Brittberg M, Lindahl A (2003) Autologous chondrocyte transplantation of the ankle. Foot Ankle Clin 8:291–303
17. Peterson L, Brittberg M, Kiviranta I et al (2002) Autologous chondrocyte transplantation. Biomechanics and long-term durability. Am J Sports Med 30:2–12
18. Peterson L, Minas T, Brittberg M et al (2003) Treatment of osteochondritis dissecans of the knee with autologous chondrocyte transplantation: results at two to ten years. J Bone Joint Surg Am 85-A(Suppl 2):17–24
19. Peterson L, Minas T, Brittberg M et al (2000) Two- to 9-year outcome after autologous chondrocyte transplantation of the knee. Clin Orthop Relat Res 374:212–234
20. Brittberg M (1999) Autologous chondrocyte transplantation. Clin Orthop Relat Res 367(Suppl):S147–S155
21. Brittberg M, Lindahl A, Homminga G et al (1997) A critical analysis of cartilage repair. Acta Orthop Scand 68:186–191
22. Knutsen G, Engebretsen L, Ludvigsen TC et al (2004) Autologous chondrocyte implantation compared with microfracture in the knee. A randomized trial. J Bone Joint Surg Am 86-A:455–464
23. Kreuz PC, Erggelet C, Steinwachs MR et al (2006) Is microfracture of chondral defects in the knee associated with different results in patients aged 40 years or younger? Arthroscopy 22:1180–1186
24. Kreuz PC, Steinwachs MR, Erggelet C et al (2006) Results after microfracture of full-thickness chondral defects in different compartments in the knee. Osteoarthr Cartil 14:1119–1125
25. Szerb I, Hangody L, Duska Z et al (2005) Mosaicplasty: long-term follow-up. Bull Hosp Jt Dis 63:54–62
26. Henderson I, Tuy BOakes B (2004) Reoperation after autologous chondrocyte implantation. Indications and findings. J Bone Joint Surg Br 86:205–211
27. Nehrer S, Minas T (2000) Treatment of articular cartilage defects. Invest Radiol 35:639–46
28. Nehrer S, Breinan HA, Ramappa A et al (1998) Chondrocyte-seeded collagen matrices implanted in a chondral defect in a canine model. Biomaterials 19:2313–2328
29. Dorotka R, Windberger U, Macfelda K et al (2005) Repair of articular cartilage defects treated by microfracture and a three-dimensional collagen matrix. Biomaterials 26:3617–629
30. Dorotka R, Bindreiter U, Macfelda K et al (2005) Marrow stimulation and chondrocyte transplantation using a collagen matrix for cartilage repair. Osteoarthr Cartil 13:655–664
31. Cortivo R, Brun P, Rastrelli A et al (1991) In vitro studies on biocompatibility of hyaluronic acid esters. Biomaterials 12:727–730
32. Campoccia D, Doherty P, Radice M et al (1998) Semisynthetic resorbable materials from hyaluronan esterification. Biomaterials 19:2101–2127
33. Nehrer S, Domayer S, Dorotka R et al (2006) Three-year clinical outcome after chondrocyte transplantation using a hyaluronan matrix for cartilage repair. Eur J Radiol 57:3–8
34. Pavesio A, Abatangelo G, Borrione A et al (2003) Hyaluronan-based scaffolds (Hyalograft C) in the treatment of knee cartilage defects: preliminary clinical findings. Novartis Found Symp 249:203–217, discussion 229–33, 234–8, 239–241
35. Chu CR, Coutts RD, Yoshioka M et al (1995) Articular cartilage repair using allogeneic perichondrocyte-seeded biodegradable porous polylactic acid (PLA): a tissue-engineering study. J Biomed Mater Res 29:1147–1154
36. Behrens P, Bitter T, Kurz B et al (2006) Matrix-associated autologous chondrocyte transplantation/implantation (MACT/MACI)—5-year follow-up. Knee 13:194–202
37. Steinwachs M, Kreuz PC (2007) Autologous chondrocyte implantation in chondral defects of the knee with a type I/III collagen membrane: a prospective study with a 3-year follow-up. Arthroscopy 23:381–387
38. Marcacci M, Berruto M, Brocchetta D et al (2005) Articular cartilage engineering with Hyalograft C: 3-year clinical results. Clin Orthop Relat Res 435:96–105

39. Marcacci M, Zaffagnini S, Kon E et al (2002) Arthroscopic autologous chondrocyte transplantation: technical note. Knee Surg Sports Traumatol Arthrosc 10:154–159
40. Grigolo B, Lisignoli G, Piacentini A et al (2002) Evidence for redifferentiation of human chondrocytes grown on a hyaluronan-based biomaterial (HYAff 11): molecular, immunohistochemical and ultrastructural analysis. Biomaterials 23:1187–1195
41. Eckstein F, Hudelmaier M, Wirth W et al (2006) Double echo steady state magnetic resonance imaging of knee articular cartilage at 3 Tesla: a pilot study for the Osteoarthritis Initiative. Ann Rheum Dis 65:433–441
42. Link TM, Majumdar S, Peterfy C et al (1998) High resolution MRI of small joints: impact of spatial resolution on diagnostic performance and SNR. Magn Reson Imaging 16:147–155
43. Rubenstein JD, Li JG, Majumdar S et al (1997) Image resolution and signal-to-noise ratio requirements for MR imaging of degenerative cartilage. AJR Am J Roentgenol 169:1089–1096
44. Peterfy CG, Guermazi A, Zaim S et al (2004) Whole-organ magnetic resonance imaging score (WORMS) of the knee in osteoarthritis. Osteoarthr Cartil 12:177–190
45. Kornaat PR, Ceulemans RY, Kroon HM et al (2005) MRI assessment of knee osteoarthritis: Knee Osteoarthritis Scoring System (KOSS)—inter-observer and intra-observer reproducibility of a compartment-based scoring system. Skeletal Radiol 34:95–102
46. Conaghan PGHD, Tennant A, Amin S, Clancy M, Guermazi A et al (2004) Evaluation an MRI scoring system for osteoarthritis of the knee using modern psychometric approaches. Osteoarthr Cartil 12(Suppl B):118 [abstract]
47. Hunter DJ, Lo GH, Gale D et al (2008) The reliability of a new scoring system for knee osteoarthritis MRI and the validity of bone marrow lesion assessment: BLOKS (Boston Leeds Osteoarthritis Knee Score). Ann Rheum Dis 67:206–211
48. Yoshioka H, Stevens K, Hargreaves BA et al (2004) Magnetic resonance imaging of articular cartilage of the knee: comparison between fat-suppressed three-dimensional SPGR imaging, fat-suppressed FSE imaging, and fat-suppressed three-dimensional DEFT imaging, and correlation with arthroscopy. J Magn Reson Imaging 20:857–864
49. Mohr A, Priebe M, Taouli B et al (2003) Selective water excitation for faster MR imaging of articular cartilage defects: initial clinical results. Eur Radiol 13:686–689
50. Kawahara Y, Uetani M, Nakahara N et al (1998) Fast spin-echo MR of the articular cartilage in the osteoarthrotic knee. Correlation of MR and arthroscopic findings. Acta Radiol 39:120–125
51. Broderick LS, Turner DA, Renfrew DL et al (1994) Severity of articular cartilage abnormality in patients with osteoarthritis: evaluation with fast spin-echo MR vs arthroscopy. AJR Am J Roentgenol 162:99–103
52. Disler DG, McCauley TR, Kelman CG et al (1996) Fat-suppressed three-dimensional spoiled gradient-echo MR imaging of hyaline cartilage defects in the knee: comparison with standard MR imaging and arthroscopy. AJR Am J Roentgenol 167:127–132
53. Recht MP, Kramer J, Marcelis S et al (1993) Abnormalities of articular cartilage in the knee: analysis of available MR techniques. Radiology 187:473–478
54. Recht MP, Piraino DW, Paletta GA et al (1996) Accuracy of fat-suppressed three-dimensional spoiled gradient-echo FLASH MR imaging in the detection of patellofemoral articular cartilage abnormalities. Radiology 198:209–212
55. Bredella MA, Tirman PF, Peterfy CG et al (1999) Accuracy of T2-weighted fast spin-echo MR imaging with fat saturation in detecting cartilage defects in the knee: comparison with arthroscopy in 130 patients. AJR Am J Roentgenol 172:1073–1080
56. Masi JN, Sell CA, Phan C et al (2005) Cartilage MR imaging at 3.0 versus that at 1.5 T: preliminary results in a porcine model. Radiology 236:140–150
57. Link TM, Sell CA, Masi JN et al (2006) 3.0 vs 1.5 T MRI in the detection of focal cartilage pathology—ROC analysis in an experimental model. Osteoarthr Cartil 14:63–70
58. Lee KY, Masi JN, Sell CA et al (2005) Computer-aided quantification of focal cartilage lesions using MRI: accuracy and initial arthroscopic comparison. Osteoarthr Cartil 13:728–737
59. McGibbon CA, Trahan CA (2003) Measurement accuracy of focal cartilage defects from MRI and correlation of MRI graded lesions with histology: a preliminary study. Osteoarthr Cartil 11:483–493
60. Graichen H, Al-Shamari D, Hinterwimmer S et al (2005) Accuracy of quantitative magnetic resonance imaging in the detection of ex vivo focal cartilage defects. Ann Rheum Dis 64:1120–1125
61. Marlovits S, Trattnig S (2006) Cartilage repair. Eur J Radiol 57:1–2
62. Marlovits S, Singer P, Zeller P et al (2006) Magnetic resonance observation of cartilage repair tissue (MOCART) for the evaluation of autologous chondrocyte transplantation: determination of interobserver variability and correlation to clinical outcome after 2 years. Eur J Radiol 57:16–23
63. Trattnig S, Millington SA, Szomolanyi P et al (2007) MR imaging of osteochondral grafts and autologous chondrocyte implantation. Eur Radiol 17:103–118
64. Trattnig S, Ba-Ssalamah A, Pinker K et al (2005) Matrix-based autologous chondrocyte implantation for cartilage repair: noninvasive monitoring by high-resolution magnetic resonance imaging. Magn Reson Imaging 23:779–787
65. Winalski CS, Gupta KB (2003) Magnetic resonance imaging of focal articular cartilage lesions. Top Magn Reson Imaging 14:131–144
66. Brittberg M, Winalski CS (2003) Evaluation of cartilage injuries and repair. J Bone Joint Surg Am 85-A (Suppl 2):58–69
67. Trattnig S, Pinker K, Krestan C et al (2006) Matrix-based autologous chondrocyte implantation for cartilage repair with HyalograftC: two-year follow-up by magnetic resonance imaging. Eur J Radiol 57:9–15
68. Weissleder R, Mahmood U (2001) Molecular imaging. Radiology 219:316–333
69. Trattnig S, Mamisch TC, Welsch GH et al (2007) Quantitative T2 mapping of matrix-associated autologous chondrocyte transplantation at 3 Tesla: an in vivo cross-sectional study. Invest Radiol 42:442–448
70. Trattnig S, Marlovits S, Gebetsroither S et al (2007) Three-dimensional delayed gadolinium-enhanced MRI of cartilage (dGEMRIC) for in vivo evaluation of reparative cartilage after matrix-associated autologous chondrocyte transplantation at 3.0T: preliminary results. J Magn Reson Imaging 26:974–982
71. Watanabe A, Wada Y, Obata T et al (2005) Time course evaluation of reparative cartilage with MR imaging after autologous chondrocyte implantation. Cell Transplant 14:695–700
72. Glaser C, Mendlik T, Dinges J et al (2006) Global and regional reproducibility of T2 relaxation time measurements in human patellar cartilage. Magn Reson Med 56:527–534

73. Mosher TJ, Dardzinski BJ (2004) Cartilage MRI T2 relaxation time mapping: overview and applications. Semin Musculoskelet Radiol 8:355–368
74. Burstein D, Gray ML (2006) Is MRI fulfilling its promise for molecular imaging of cartilage in arthritis? Osteoarthr Cartil 14:1087–1090
75. Lusse S, Claassen H, Gehrke T et al (2000) Evaluation of water content by spatially resolved transverse relaxation times of human articular cartilage. Magn Reson Imaging 18:423–430
76. Menezes NM, Gray ML, Hartke JR et al (2004) T2 and T1rho MRI in articular cartilage systems. Magn Reson Med 51:503–509
77. Nieminen MT, Rieppo J, Toyras J et al (2001) T2 relaxation reveals spatial collagen architecture in articular cartilage: a comparative quantitative MRI and polarized light microscopic study. Magn Reson Med 46:487–493
78. Xia Y, Moody JB, Alhadlaq H (2002) Orientational dependence of T2 relaxation in articular cartilage: A microscopic MRI (microMRI) study. Magn Reson Med 48:460–469
79. Dardzinski BJ, Mosher TJ, Li S et al (1997) Spatial variation of T2 in human articular cartilage. Radiology 205:546–550
80. Watrin-Pinzano A, Ruaud JP, Cheli Y et al (2004) Evaluation of cartilage repair tissue after biomaterial implantation in rat patella by using T2 mapping. Magma 17:219–228
81. Goodwin DW, Wadghiri YZDunn JF (1998) Micro-imaging of articular cartilage: T2, proton density, and the magic angle effect. Acad Radiol 5:790–798
82. Goodwin DW, Zhu HDunn JF (2000) In vitro MR imaging of hyaline cartilage: correlation with scanning electron microscopy. AJR Am J Roentgenol 174:405–409
83. Grunder W (2006) MRI assessment of cartilage ultrastructure. NMR Biomed 19:855–876
84. Nissi MJ, Rieppo J, Toyras J et al (2006) T(2) relaxation time mapping reveals age- and species-related diversity of collagen network architecture in articular cartilage. Osteoarthr Cartil 14:1265–1271
85. Shinar H, Navon G (2006) Multinuclear NMR and microscopic MRI studies of the articular cartilage nanostructure. NMR Biomed 19:877–893
86. Goebel JC, Watrin-Pinzano A, Bettembourg-Brault I et al (2006) Age-related quantitative MRI changes in healthy cartilage: preliminary results. Biorheology 43:547–551
87. Mosher TJ, Dardzinski BJ, Smith MB (2000) Human articular cartilage: influence of aging and early symptomatic degeneration on the spatial variation of T2—preliminary findings at 3 T. Radiology 214:259–266
88. Mosher TJ, Liu Y, Yang QX et al (2004) Age dependency of cartilage magnetic resonance imaging T2 relaxation times in asymptomatic women. Arthritis Rheum 50:2820–2828
89. White LM, Sussman MS, Hurtig M et al (2006) Cartilage T2 assessment: differentiation of normal hyaline cartilage and reparative tissue after arthroscopic cartilage repair in equine subjects. Radiology 241:407–414
90. Welsch GH, Mamisch TC, Domayer S, Dorotka R, Kutsch-Lissberg F, Marlovits S, White L, Trattnig S (2008) Cartilage T2 assessment at 3 Tesla: in vivo differentiation of normal hyaline cartilage and reparative tissue in patients after two different cartilage repair procedures - initial experiences. Radiology 247(1):154–161
91. Gobbi A, Nunag P, Malinowski K (2005) Treatment of full thickness chondral lesions of the knee with microfracture in a group of athletes. Knee Surg Sports Traumatol Arthrosc 13:213–221
92. Domayer SE, Kutscha-Lissberg F, Welsch GH, et al (2008) T2 mapping in the knee after microfracture at 3.0 T: correlation of global T2 values and clinical outcome - preliminary results. Osteoarthr Cartil 16:903–908 doi:10.1016/j.joca.2007.11.014
93. Kurkijarvi JE, Mattila L, Ojala RO et al (2007) Evaluation of cartilage repair in the distal femur after autologous chondrocyte transplantation using T2 relaxation time and dGEMRIC. Osteoarthr Cartil 15:372–378
94. Lohmander LS (1994) Articular cartilage and osteoarthrosis. The role of molecular markers to monitor breakdown, repair and disease. J Anat 184(Pt 3):477–492
95. Bashir A, Gray ML, Hartke J et al (1999) Nondestructive imaging of human cartilage glycosaminoglycan concentration by MRI. Magn Reson Med 41:857–865
96. Burstein D, Velyvis J, Scott KT et al (2001) Protocol issues for delayed Gd(DTPA)(2-)-enhanced MRI (dGEMRIC) for clinical evaluation of articular cartilage. Magn Reson Med 45:36–41
97. Kim YJ, Jaramillo D, Millis MB et al (2003) Assessment of early osteoarthritis in hip dysplasia with delayed gadolinium-enhanced magnetic resonance imaging of cartilage. J Bone Joint Surg Am 85-A:1987–1992
98. Tiderius CJ, Olsson LE, Leander P et al (2003) Delayed gadolinium-enhanced MRI of cartilage (dGEMRIC) in early knee osteoarthritis. Magn Reson Med 49:488–492
99. Roos EM, Dahlberg L (2005) Positive effects of moderate exercise on glycosaminoglycan content in knee cartilage: a four-month, randomized, controlled trial in patients at risk of osteoarthritis. Arthritis Rheum 52:3507–514
100. McKenzie CA, Williams A, Prasad PV et al (2006) Three-dimensional delayed gadolinium-enhanced MRI of cartilage (dGEMRIC) at 1.5T and 3.0T. J Magn Reson Imaging 24:928–933
101. Kimelman T, Vu A, Storey P et al (2006) Three-dimensional T1 mapping for dGEMRIC at 3.0 T using the Look Locker method. Invest Radiol 41:198–203
102. Watanabe A, Wada Y, Obata T et al (2006) Delayed gadolinium-enhanced MR to determine glycosaminoglycan concentration in reparative cartilage after autologous chondrocyte implantation: preliminary results. Radiology 239:201–208
103. Wayne JS, Kraft KA, Shields KJ et al (2003) MR imaging of normal and matrix-depleted cartilage: correlation with biomechanical function and biochemical composition. Radiology 228:493–499
104. Gillis A, Bashir A, McKeon B et al (2001) Magnetic resonance imaging of relative glycosaminoglycan distribution in patients with autologous chondrocyte transplants. Invest Radiol 36:743–748
105. Tins BJ, McCall IW, Takahashi T et al (2005) Autologous chondrocyte implantation in knee joint: MR imaging and histologic features at 1-year follow-up. Radiology 234:501–508
106. Trattnig S, Mamisch TC, Pinker K, Domayer S, Szomolanyi P, Marlovits S, Kutscha-Lissberg F, Welsch GH (2008) Differentiating normal hyaline cartilage from post-surgical repair tissue using fast gradient echo imaging in delayed gadolinium enhanced MRI - (dGEMRIC) at 3 Tesla. Eur Radiol 18 (6):1251–1259
107. Minas T, Nehrer S (1997) Current concepts in the treatment of articular cartilage defects. Orthopedics 20:525–538

108. Ghivizzani SC, Oligino TJ, Robbins PD et al (2000) Cartilage injury and repair. Phys Med Rehabil Clin N Am 11:289–307
109. Kurkijarvi JE, Nissi MJ, Kiviranta I et al (2004) Delayed gadolinium-enhanced MRI of cartilage (dGEMRIC) and T2 characteristics of human knee articular cartilage: topographical variation and relationships to mechanical properties. Magn Reson Med 52:41–46
110. Williams A, Gillis A, McKenzie C et al (2004) Glycosaminoglycan distribution in cartilage as determined by delayed gadolinium-enhanced MRI of cartilage (dGEMRIC): potential clinical applications. AJR Am J Roentgenol 182:167–172
111. Miller KL, Hargreaves BA, Gold GE et al (2004) Steady-state diffusion-weighted imaging of in vivo knee cartilage. Magn Reson Med 51:394–398
112. Deoni SC, Peters TMRutt BK (2004) Quantitative diffusion imaging with steady-state free precession. Magn Reson Med 51:428–433
113. Mamisch TC, Menzel MI, Welsch GH et al (2008) Steady-state diffusion imaging for MR in-vivo evaluation of reparative cartilage after matrix-associated autologous chondrocyte transplantation at 3 Tesla—preliminary results. Eur J Radiol 65:72–79
114. Eckstein F, Burstein D, Link TM (2006) Quantitative MRI of cartilage and bone: degenerative changes in osteoarthritis. NMR Biomed 19:822–854
115. Eckstein F, Hudelmaier M, Putz R (2006) The effects of exercise on human articular cartilage. J Anat 208:491–512
116. Eckstein F, Cicuttini F, Raynauld JP et al (2006) Magnetic resonance imaging (MRI) of articular cartilage in knee osteoarthritis (OA): morphological assessment. Osteoarthr Cartil 14(Suppl A):A46–A75
117. Eckstein F, Ateshian G, Burgkart R et al (2006) Proposal for a nomenclature for magnetic resonance imaging based measures of articular cartilage in osteoarthritis. Osteoarthr Cartil 14:974–83
118. Glaser C, Tins BJ, Trumm CG et al (2007) Quantitative 3D MR evaluation of autologous chondrocyte implantation in the knee: feasibility and initial results. Osteoarthr Cartil 15:798–807
119. Bashir A, Gray ML, Boutin RD et al (1997) Glycosaminoglycan in articular cartilage: in vivo assessment with delayed Gd(DTPA)(2−)-enhanced MR imaging. Radiology 205:551–558
120. Nehrer S, Spector M, Minas T (1999) Histologic analysis of tissue after failed cartilage repair procedures. Clin Orthop Relat Res 365:149–162
121. Henderson I, Lavigne P, Valenzuela H et al (2007) Autologous chondrocyte implantation: superior biologic properties of hyaline cartilage repairs. Clin Orthop Relat Res 455:253–261
122. Knutsen G, Drogset JO, Engebretsen L et al (2007) A randomized trial comparing autologous chondrocyte implantation with microfracture. Findings at five years. J Bone Joint Surg Am 89:2105–2112
123. Saris DB, Vanlauwe J, Victor J et al (2008) Characterized chondrocyte implantation results in better structural repair when treating symptomatic cartilage defects of the knee in a randomized controlled trial versus microfracture. Am J Sports Med 36:235–246
124. Henderson IJTB, Connell D, Oakes B, Hettwer WH (2003) Prospective clinical study of autologous chondrocyte implantation and correlation with MRI at three and 12 months. J Bone Joint Surg Br 85:1060–1066
125. Gobbi A, Kon E, Berruto M et al (2006) Patellofemoral full-thickness chondral defects treated with Hyalograft-C: a clinical, arthroscopic, and histologic review. Am J Sports Med 34:1763–1773